



Image-charge-induced localization of molecular orbitals at metal-molecule interfaces Self-consistent GW calculations

Strange, M.; Thygesen, K. S.

Published in:
Physical Review B Condensed Matter

Link to article, DOI:
[10.1103/PhysRevB.86.195121](https://doi.org/10.1103/PhysRevB.86.195121)

Publication date:
2012

Document Version
Publisher's PDF, also known as Version of record

[Link back to DTU Orbit](#)

Citation (APA):
Strange, M., & Thygesen, K. S. (2012). Image-charge-induced localization of molecular orbitals at metal-molecule interfaces: Self-consistent GW calculations. *Physical Review B Condensed Matter*, 86(19), 195121. <https://doi.org/10.1103/PhysRevB.86.195121>

General rights

Copyright and moral rights for the publications made accessible in the public portal are retained by the authors and/or other copyright owners and it is a condition of accessing publications that users recognise and abide by the legal requirements associated with these rights.

- Users may download and print one copy of any publication from the public portal for the purpose of private study or research.
- You may not further distribute the material or use it for any profit-making activity or commercial gain
- You may freely distribute the URL identifying the publication in the public portal

If you believe that this document breaches copyright please contact us providing details, and we will remove access to the work immediately and investigate your claim.

Image-charge-induced localization of molecular orbitals at metal-molecule interfaces: Self-consistent *GW* calculations

M. Strange and K. S. Thygesen*

Center for Atomic-Scale Materials Design, Department of Physics, Technical University of Denmark, DK-2800 Kongens Lyngby, Denmark
(Received 24 April 2012; revised manuscript received 1 November 2012; published 15 November 2012)

Quasiparticle (QP) wave functions, also known as Dyson orbitals, extend the concept of single-particle states to interacting electron systems. Here we employ many-body perturbation theory in the *GW* approximation to calculate the QP wave functions for a semiempirical model describing a π -conjugated molecular wire in contact with a metal surface. We find that image charge effects pull the frontier molecular orbitals toward the metal surface, while orbitals with higher or lower energy are pushed away. This affects both the size of the energetic image charge shifts and the coupling of the individual orbitals to the metal substrate. Full diagonalization of the QP equation and, to some extent, self-consistency in the *GW* self-energy, is important to describe the effect, which is not captured by standard density functional theory or Hartree-Fock. These results should be important for the understanding and theoretical modeling of electron transport across metal-molecule interfaces.

DOI: [10.1103/PhysRevB.86.195121](https://doi.org/10.1103/PhysRevB.86.195121)

PACS number(s): 73.20.-r, 71.10.-w, 72.10.-d

I. INTRODUCTION

The independent-particle approximation and the associated one-electron orbital picture forms the basis of our understanding of chemical bonding and electronic energy levels in solids and molecules. The most widely used approximations of this type are Hartree-Fock (HF) and density functional theory (DFT).^{1,2} Although the single-particle orbitals derived from such schemes do not have physical meaning, apart from the fact that the exact DFT orbitals generate the exact ground-state density, they are routinely used to calculate and interpret physical quantities of various types. In strongly correlated systems such an approach clearly breaks down. However, even in weakly correlated systems where the single-particle picture is valid, there is no guarantee that the orbitals generated by the standard one-electron schemes are those which best resemble the true many-body excitations.

Quasiparticle (QP) wave functions provide a rigorous generalization of the concept of single-particle orbitals to interacting electron systems. The QP states and energies are solutions of the QP equation,³

$$[\hat{H}_0 + \hat{\Sigma}_{xc}(\epsilon_\mu)]|\psi_\mu\rangle = \epsilon_\mu|\psi_\mu\rangle. \quad (1)$$

Here \hat{H}_0 is the noninteracting part of the Hamiltonian including the Hartree field, while $\hat{\Sigma}_{xc}$ is the nonlocal and energy-dependent exchange-correlation (xc) self-energy operator.⁴ The QP energies represent the possible energies of a particle (electron or hole) added to the N -particle ground state, and the QP wave function describes the probability amplitude for finding the added particle at a given position. (A precise definition and interpretation of the QP energies and wave functions are given later in this paper.)

The *GW* approximation³ to Σ_{xc} (in both its self-consistent and its non-self-consistent form) has been successfully used to calculate QP energies of solids,^{6–10} molecules,^{11,12} and, more recently, solid-molecule interfaces.^{13–17} The latter class of systems is particularly challenging to describe due to its highly inhomogeneous nature where the screening changes from metallic to insulating over a few Å. Since the QP states describe the charged excitations, the QP energies of an

adsorbed molecule are strongly affected by the metal surface through long-range polarization effects (image charge effects) which decay as $1/z$, with z being the distance to the surface [see Fig. 1]. The inability of any available DFT functional to account for this renormalization of molecular energy levels reflects the highly nonlocal nature of the phenomenon. We stress that this does not imply that the single-particle picture is invalid in such cases; only that the correct QP orbitals and energies cannot be obtained from a semi-local or nonlocal exchange potential.

Most applications of the QP equation have focused on the QP *energies*, while the QP wave functions have been much less studied. In fact it is very often assumed that the latter, apart from normalization, are identical to the orbitals obtained from DFT (ψ_μ^0). Under that assumption, QP energies can be obtained from first-order perturbation theory involving only the diagonal matrix elements $\langle\psi_\mu^0|\Sigma_{xc}(\epsilon_\mu^0)|\psi_\mu^0\rangle$, thus greatly reducing the computational cost of solving the QP equation.

As an example where the shape of the QP wave functions plays a key role we consider the case of electron transport through a molecule connected to metallic electrodes. The conductance of the junction depends mainly on two factors,

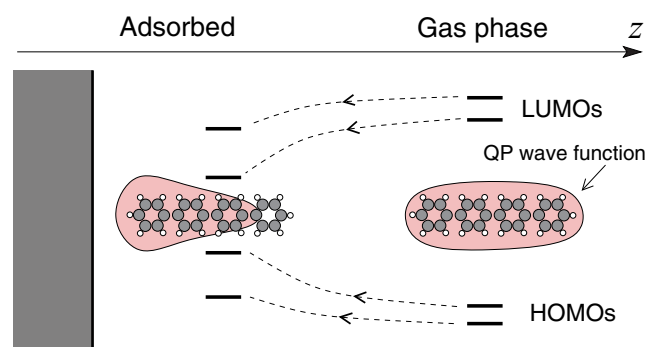


FIG. 1. (Color online) Schematic of the change in the frontier QP energies and wave functions of a molecule approaching a metal surface. The closing of the HOMO-LUMO gap due to image charge screening is associated with a change in the shape of the orbital.

namely, (i) the position of the molecule's frontier (QP) energy levels relative to the metal Fermi energy and (ii) the overlap between the molecule's frontier (QP) orbitals and the extended states in the electrodes. The importance of factor (i) has been studied in detail using scissors operator techniques to correct the DFT energy levels while keeping the DFT orbitals fixed.^{18,19} In contrast, the question of how well the DFT orbitals resemble the true QP orbitals and the consequences for charge transport have been studied only indirectly.^{20–24}

In this paper we show, using many-body perturbation theory in the *GW* approximation, that the QP wave functions of a molecular wire in contact with a metal surface can be qualitatively different from those obtained from an independent-particle approximation: While the Hartree-Fock single-particle orbitals remain delocalized over the molecule upon coupling to the surface, our *GW* calculations show that image charge effects not only cause a reduction in the QP energies as previously demonstrated, but also renormalize the molecular orbitals. Orbitals with an energy close to the Fermi level are pulled more towards the surface, while higher- and lower-lying orbitals are pushed away. As a result, not only the energies but also the lifetimes (tunneling width) of the molecular resonances are affected by the xc self-energy.

The paper is organized as follows. In Sec. II we briefly review the general QP theory including a transparent definition of the QP states and a brief discussion of the equivalence between this definition and the QP equation. In Sec. III we introduce the metal-molecule interface model and in Sec. IV we explain the method used to calculate the QP energies and wave functions. In Sec. V we present the results and discuss implications for modeling of charge transport in molecular junctions.

II. QUASIPARTICLE THEORY

In this section we review the concept of the QP wave function and discuss its physical meaning. For simplicity we make the assumption that the system under consideration is finite and the relevant excitations are discrete.²⁸

We denote the N -particle ground state and the excited states $|\Psi_0^N\rangle$ and $|\Psi_\mu^N\rangle$, respectively. The occupied and unoccupied QP orbitals are denoted $|\psi_\mu^-\rangle$ and $|\psi_\nu^+\rangle$, respectively. The QP orbitals belong to the single-particle Hilbert space and are defined through their matrix elements with a general orbital $|\phi\rangle$:

$$\langle\phi|\psi_\mu^-\rangle^* = \langle\Psi_\mu^{N-1}|\hat{c}_\phi|\Psi_0^N\rangle, \quad (2)$$

$$\langle\phi|\psi_\nu^+\rangle = \langle\Psi_\nu^{N+1}|\hat{c}_\phi^\dagger|\Psi_0^N\rangle, \quad (3)$$

where \hat{c}_ϕ and \hat{c}_ϕ^\dagger annihilates and creates an electron in the orbital $|\phi\rangle$, respectively. The real-space representation of the QP wave functions are obtained by setting $|\phi\rangle = |r\rangle$ in the above equations. The QP wave functions defined above are also sometimes referred to as Lehman amplitudes or Dyson orbitals.

The QP energies are defined by

$$\varepsilon_\mu^- = E_0^N - E_\mu^{N-1}, \quad (4)$$

$$\varepsilon_\nu^+ = E_\nu^{N+1} - E_0^N. \quad (5)$$

They represent the excitation energies of the $N \pm 1$ relative to E_0^N and thus correspond to electron addition/removal energies.

The definition of the QP wave functions given in Eqs. (2) and (3) is not very transparent at first sight. A more transparent definition of the QP states can be obtained by noting that the projection

$$\frac{|\langle\Psi_\mu^{N+1}|\hat{c}_\phi^\dagger|\Psi_0^N\rangle|^2}{\langle\phi|\phi\rangle} \quad (6)$$

is maximized exactly when $|\phi\rangle = |\psi_\mu^+\rangle$. In other words, $|\psi_\mu^+\rangle$ is the orbital that makes $\hat{c}_\phi^\dagger|\Psi_0^N\rangle$ the best approximation to the excited state $|\Psi_\mu^{N+1}\rangle$. Similarly, $|\psi_\mu^-\rangle$ is the orbital that makes $\hat{c}_\phi|\Psi_0^N\rangle$ the best approximation to the excited state $|\Psi_\mu^{N-1}\rangle$. Consequently, the QP wave function is the single-particle orbital that best describes the state of the “extra” electron/hole in the excited state $|\Psi_\mu^{N\pm 1}\rangle$. In general, the QP states are nonorthogonal and their norm lies between 0 and 1. The norm is a measure of how well the excited many-body state can be described as a single-particle excitation from the ground state.

In the special case of noninteracting electrons, the QP wave functions have norms of exactly 1 or 0. The former correspond to excitations where one extra particle has been added to the ground-state Slater determinant. In this case the QP wave functions coincide with the normalized eigenstates of the one-electron Hamiltonian. The QP states with 0 norm correspond to all other types of excitations.

It should be noted that the term “quasiparticle state” is often used only for those $|\psi_\mu^{+/-}\rangle$ whose norm is close to 1, while other states (those corresponding to collective excitations) are referred to as “satellites.” In the present work we only consider QP states with norms very close to 1.

In the case where $E_\mu^{N\pm 1}$ belongs to the discrete spectrum of the many-body Hamiltonian, it can be shown that ψ_μ^\pm and ε_μ^\pm are solutions to the QP equation, (1). In this case the norm of the QP state is given by $Z = (1 - d\Sigma_{xc}(\varepsilon_\mu^\pm)/d\varepsilon)^{-1}$. The definition of QP states belonging to the continuum is a bit trickier,²⁸ but this has no consequences for the present work.

III. MODEL

We consider a four-unit paraphenylene molecular wire connected to a metal surface (see Fig. 2). The paraphenylene molecule is described by a Pariser-Parr-Pople (PPP) Hamiltonian,²⁵

$$\hat{H}_\pi = \sum_{\langle ij \rangle, \sigma} t \hat{c}_{i\sigma}^\dagger \hat{c}_{j\sigma} + \frac{1}{2} \sum_{ij, \sigma\sigma'} V_{ij} \hat{c}_{i\sigma}^\dagger \hat{c}_{j\sigma'}^\dagger \hat{c}_{j\sigma'} \hat{c}_{i\sigma}, \quad (7)$$

where $\hat{c}_{i\sigma}^\dagger$ ($\hat{c}_{i\sigma}$) creates (annihilates) an electron at site i (p_z orbital of carbon atom i) with spin σ . The first term describes nearest-neighbor hopping of strength $t = -2.4$ eV. In the second term, V_{ij} is the long-range Coulomb interaction acting between all sites on the molecule and for which we use Ohno's parametrization,²⁶

$$V_{ij} = \frac{14.4}{\sqrt{(14.4/U)^2 + R_{ij}^2}}, \quad (8)$$

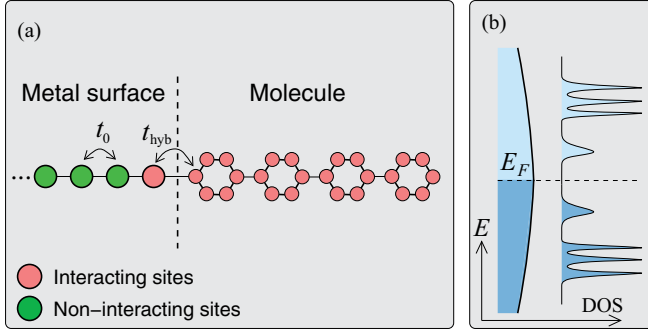


FIG. 2. (Color online) (a) Lattice model of a molecular wire interacting with a metal surface via hopping and Coulomb interaction. (b) QP density of states (spectral function) of the adsorbed molecule. The different broadening of the levels reflects the difference in the shape of the QP orbitals.

where R_{ij} is the distance between atom i and atom j (in Å) and $U = 11.26$ (in eV). We note that the PPP model with the parameters used here, in general, provides an accurate description of the low-lying excitations in π -conjugated systems.²⁷

As a qualitative model of the metal surface we use a semi-infinite one-dimensional tight-binding lattice. We use the large hopping parameter of $t_0 = -5.0$ eV between the sites of the chain to simulate a broad featureless band and we set $E_F = 0$ corresponding to half-filling. The last site on the metallic chain is coupled to the nearest carbon atom of the molecule by the hopping parameter $t_{\text{hyb}} = 1.0$ eV (see inset in Fig. 4). Coulomb interactions, V_{ij} , as defined in Eq. (8) are included between the last site on the chain and all the sites of the molecule. We set the distance between the last site of the chain and the contacting carbon atom to 1.5 Å. With these parameters, the model yields realistic image charge shifts in the range 0.2–1.0 eV, depending on the spatial form of the orbital.^{18,19} We stress that the Fermi energy lies in the middle of the gap between the highest occupied molecular orbital (HOMO) and the lowest unoccupied molecular orbital (LUMO) such that the contacted molecule remains in a closed-shell configuration far from the strong-correlation Kondo regime.

We note that the use of a one-dimensional chain to simulate the metal surface is clearly not adequate for quantitative computations. In particular, it cannot be used to describe the reorganization of electrons in the metal surface. However, from the viewpoint of the molecule, it captures, at least qualitatively, all the aspects of the image charge effect in a real metal-molecule junction: in particular, the effect that a charge added to the molecule induces an image charge in the metal (change in the occupation of the last site in the one-dimensional chain) which acts back on the electrons of the molecule. We also note that Δ -SCF as well as *ab initio* GW calculations for an alkane-diamine molecule adsorbed on an adatom, or a small pyramid tip structure, on a gold surface have shown that the image charge induced in the metal is largely confined to the adatom and is thus quite localized (see Fig. 1 in Ref. 21).

IV. METHOD

To obtain the QP wave functions and energies we calculate the single-particle Green function following the method described in Ref. 20. Briefly, the Green function of the contacted molecule is calculated from

$$G_{ij}(\omega) = [\omega - H_0 - \Sigma_{\text{hyb}}(\omega) - \Sigma_{\text{xc}}(\omega)]_{ij}^{-1}, \quad (9)$$

where H_0 is the noninteracting part of the molecular Hamiltonian including the Hartree field and Σ_{hyb} is an embedding self-energy accounting for the coupling to the semi-infinite chain. In this work the xc self-energy is evaluated using either the HF or the GW approximation. Unless explicitly stated, the GW self-energy is evaluated fully self-consistently. The energy dependence of G and Σ_{GW} is sampled on a uniform grid $\omega_n = \varepsilon_n + i\eta$, where $\eta = 0.01$ is an imaginary infinitesimal and ε_n ranges from -100 to 100 eV, with a spacing of $\eta/2 = 0.005$.

We have previously shown that the GW approximation yields QP energies of molecules described by PPP models, in good agreement with exact diagonalization results, with an average deviation of the lowest QP energies of less than 5%.³⁰ In that work we also showed, using a measure for the degree of correlation based on the entropy of the reduced density matrix, that PPP models are significantly less correlated than Hubbard models with the same interaction strengths (obtained by removing all interactions V_{ij} with $i \neq j$ from the PPP model), explaining earlier studies which concluded that GW does not perform well for Hubbard clusters.^{31,32}

The Green function is related to the QP states and energies via its Lehmann representation.⁵ Using this representation, the spectral function, $A(\omega) = (i/2\pi)[G(\omega + i\eta) - G(\omega - i\eta)]$, projected onto sites (i, j) of the molecule can be written as

$$A_{ij}(\omega) = \sum_{s \in \{+, -\}} \sum_{\mu} \langle i | \psi_{\mu}^s \rangle \langle \psi_{\mu}^s | j \rangle \delta(\omega - \varepsilon_{\mu}^s). \quad (10)$$

We identify the molecular QP energies, $\varepsilon_n^{\text{mol}}$, of the molecule as the peaks in $A(\omega)$. The corresponding QP orbital (precisely, the projection of the QP orbital of the infinite metal-molecule system onto the molecule) is obtained as the unique solution to the eigenvalue equation,

$$\sum_{j \in \text{mol}} A_{ij}(\varepsilon_n^{\text{mol}}) \langle j | \psi_n^{\text{mol}} \rangle = \lambda \langle i | \psi_n^{\text{mol}} \rangle, \quad (11)$$

with $\lambda \neq 0$. In other words, the QP orbitals are obtained by diagonalizing matrix A at its peak energies and picking the eigenvector corresponding to the largest eigenvalue (in practice, we find that the largest eigenvalue is about 10^3 times larger than the second largest). We stress that this method of obtaining the QP wave functions is equivalent to solving the QP equation, (1), but is more convenient for systems with open boundaries.

V. RESULTS

In Fig. 3 we show the band structure of the infinite poly-paraphenylene wire obtained from a DFT-LDA calculation (red) and the PPP model with interactions described at the Hartree level (blue). We have verified that the LDA xc potential

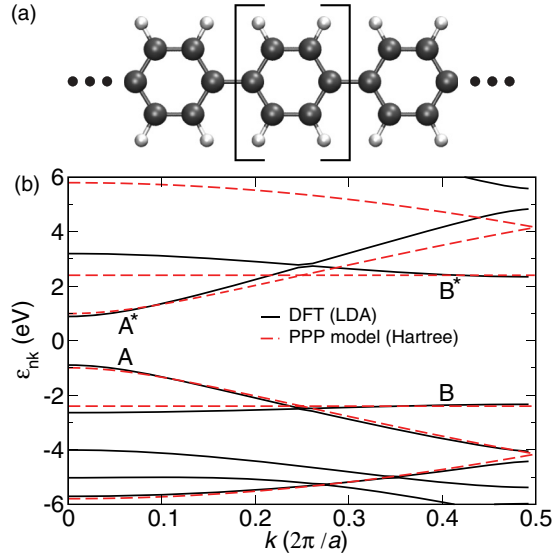


FIG. 3. (Color online) (a) Polyparaphenylene molecular wire. (b) Band structure of the infinite polyparaphenylene molecular wire calculated with the DFT(LDA) and the PPP model Hamiltonian with interactions treated at the Hartree level, respectively. The two highest valence bands (A and B) and two lowest conduction bands (A* and B*) are indicated.

merely provides a constant shift of all the bands, and thus the two levels of approximation are directly comparable. We conclude that the PPP model yields a reliable description of the π bands of polyparaphenylene. The bands denoted A and A* are mainly composed of the HOMO and LUMO orbitals of the benzene units, while the narrow B and B* bands are formed by the HOMO - 1 and LUMO + 1 benzene orbitals, respectively.

In Fig. 4 we show the projected density of states (PDOS) of the four-unit paraphenylene molecule coupled to the metallic

chain,

$$\text{PDOS}(\varepsilon) = \sum_{i \in \text{mol}} A_{ii}(\varepsilon). \quad (12)$$

For five molecular levels we indicate the shift due to correlations (mainly the image charge effect) by horizontal arrows. The single-particle orbitals obtained from HF are shown on the left, while the QP orbitals from GW are shown on the right. The weight of all the depicted QP orbitals is very close to 1 and they are essentially orthogonal, indicating that the single-particle picture applies.

The HF orbitals are completely delocalized over the molecule and are essentially identical to the orbitals of the free molecule. This is in sharp contrast to the orbitals derived from GW, which are localized on different parts of the molecule. The localization of the QP wave functions occurs because of the interaction between the hole on the molecule and the image charge that it induces in the metal surface. This is a highly nonlocal correlation effect and is completely missed by the HF approximation.

It is clear that the orbitals belonging to the narrower B band become more localized than the orbitals belonging to the wider A band. This is because it is energetically cheaper to redistribute the orbitals of a narrow band. Focusing on the B1–B4 states we observe a clear trend in the localization: The closer the energy of an orbital is to E_F , the closer to the surface the orbital is localized. Due to the image charge effect it is always energetically favorable for the hole to reside closer to the surface. On the other hand, the QP orbitals should remain (almost) orthogonal, at least when the QP picture applies as is the case here, and this prevents all orbitals from contracting towards the surface. We recall from Eq. (4) that occupied QP orbitals, ψ_μ^- , lying closer to E_F correspond to many-body excitations, Ψ_μ^{N-1} , with a lower energy. The observed trend in the localization then follows from the variational principle applied to the many-body states Ψ_μ^{N-1} .

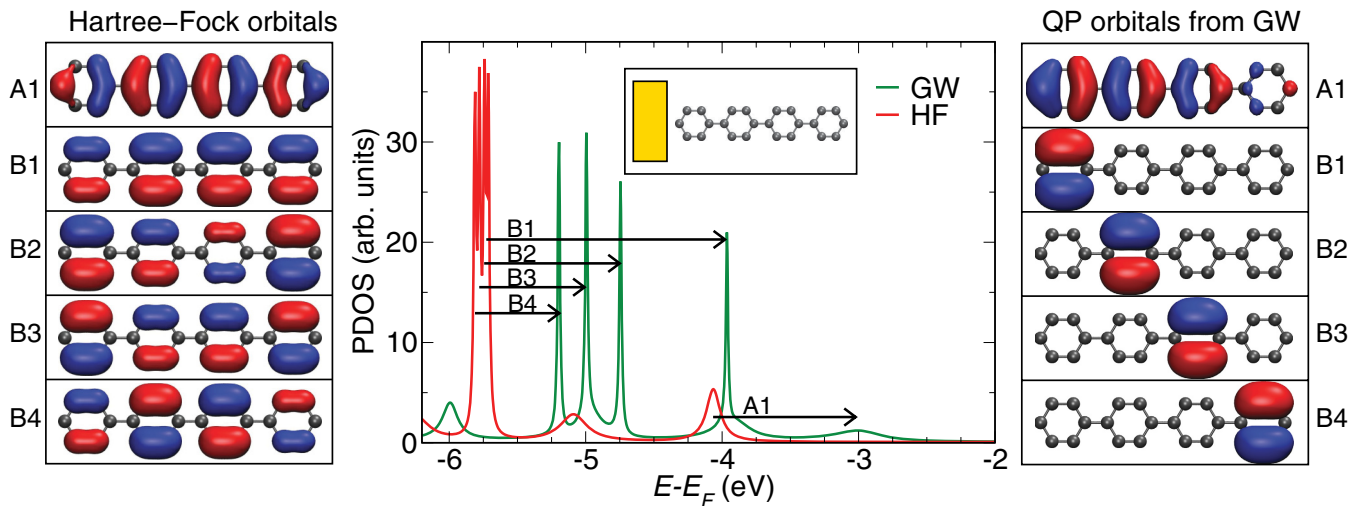


FIG. 4. (Color online) Projected density of states (PDOS) of a four-unit paraphenylene molecular wire coupled to a metal surface (middle panel). Red and green curves show results obtained at the Hartree-Fock and GW level, respectively. For five energy levels the shift due to correlations (mainly the image charge effect) is indicated by arrows, and the corresponding orbitals are plotted in the left (Hartree-Fock) and right (GW) panels. Orbital A1 is the HOMO and belongs to band A in Fig. 3, while orbitals B1–B4 belong to the narrow band B. The orbitals were constructed by superimposing p_z orbitals with weights given by the discrete wave functions of the model.

The unoccupied orbitals are affected by the metal surface in a similar way, with orbitals lying closer to E_F becoming localized more towards the surface and experiencing a larger energy shift toward E_F . The fact that the sign of the image charge shift of the energy of empty and occupied orbitals is different shows that the effect cannot be mimicked by a local $-1/z$ potential. Such a potential would shift all orbitals in the same direction (downwards). To mimic the image charge potential would instead require a nonlocal potential of the form

$$\hat{V}_{\text{img}} \sim 1/z \hat{P}_{\text{occ}} - 1/z \hat{P}_{\text{empty}}, \quad (13)$$

where \hat{P}_{occ} and \hat{P}_{empty} project onto the subspace of occupied and unoccupied molecular orbitals, respectively. From this property of the image charge potential, it is clear that the effects presented in Fig. 4 cannot be captured by a local potential.

From Fig. 4 we see that not only the QP peak positions but also the width of the resonances is affected by the image charge effect. This is particularly pronounced for the A1 orbital, which becomes significantly broadened due to the increased weight of the orbital at the carbon atom connected to the metallic chain. For the B orbitals, which have very little weight on the contacting carbon atom, the small increase in the GW peak width relative to HF comes from the (small) imaginary part of the GW self-energy.

The QP energies include correlations in addition to the exchange effects described at the HF level. The correlation energy contains contributions from the Coulomb interactions internally on the molecule (internal screening) as well as the interactions between metal and molecule (image charge screening). From calculations for the molecule in the gas phase we have verified that the contribution from internal screening is almost the same (between 0.4 and 0.6 eV) for the different molecular orbitals. Hence, apart from this constant, the difference between the QP energy and the HF energy represents the shift in the energy level due to the image charge effect.

In Fig. 5 we plot the image charge shift for the A and B orbitals versus the center of the QP orbital along the axis of the molecule, $\langle x \rangle$.

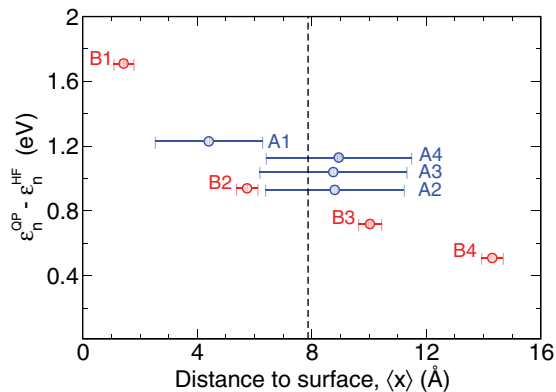


FIG. 5. (Color online) The size of the image charge effect is plotted for orbitals A1–A4 and B1–B4 versus the center of the QP orbital along the axis of the molecule, $\langle x \rangle$. The degree of localization quantified as the second moment, $\langle (x - \langle x \rangle)^2 \rangle$, is indicated by a horizontal line for each orbital. The dashed line indicates the center of the molecule. The center of all the single-particle HF orbitals fall on this line.

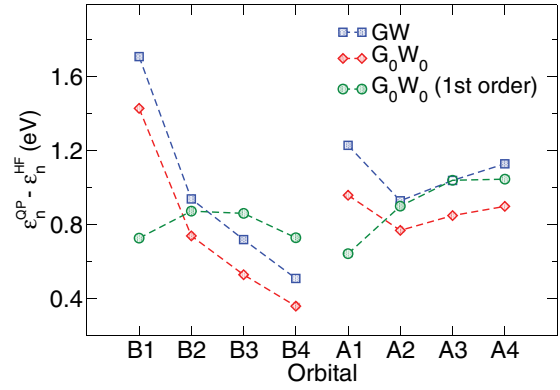


FIG. 6. (Color online) Image charge shift for the A and B orbitals calculated using three methods for calculating the GW self-energy and solving the QP equation (see text).

the molecule (the x axis). The center is defined as the first moment, $\langle \psi_n^{\text{mol}} | \hat{x} | \psi_n^{\text{mol}} \rangle$. The vertical dashed line indicates the center of the molecule, which coincides with the center of the HF orbitals. For each orbital, the degree of localization, quantified as the second moment, $\langle \psi_n^{\text{mol}} | (x - \langle x \rangle)^2 | \psi_n^{\text{mol}} \rangle$, is indicated by a horizontal line. As expected, there is a clear correlation between the size of the image charge shift and the orbital center, in particular, for the highly localized B orbitals. Orbitals A2–A4 are all pushed slightly away from the surface.

Figure 6 compares the image charge shifts obtained using three strategies for calculating the GW self-energy and solving the QP equation: (i) full solution of the QP equation with a self-consistent GW self-energy, (ii) full solution of the QP equation with a one-shot G_0W_0 self-energy with G_0 from HF, and (iii) first-order perturbation theory applied to the G_0W_0 self-energy, i.e., $\epsilon_n^{\text{QP}} = \epsilon_n^{\text{HF}} + \langle \psi_n^{\text{HF}} | \Sigma_{G_0W_0}(\epsilon_n^{\text{HF}}) - \Sigma_x | \psi_n^{\text{HF}} \rangle$, where Σ_x is the nonlocal exchange potential. As expected, the first-order approximation (iii) does not perform well in cases where the QP orbitals deviate significantly from the HF orbitals, i.e., for B1–B4 and A1. In particular, for the B1–B4 orbitals the first-order approach predicts similar image charge shifts, whereas the shifts obtained with methods i and ii vary due to the variation in the distance of the QP orbitals from the surface. As a general trend, the self-consistent treatment of the GW self-energy leads to larger image charge shifts (smaller HOMO-LUMO gaps), in agreement with findings for isolated molecules.³⁰

At first sight it might seem surprising that the image charge effect, which is essentially electrostatic in nature, is not captured by mean-field theories such as HF. The reason is that the effective potential defining the mean-field Hamiltonian does not “know” how an additional particle on the molecule becomes screened by the metal. Under some limiting conditions, however, the effect of image charge interaction can be simulated using mean-field methods to compute the total energy with an extra particle explicitly present on the molecule.^{33,34}

VI. CONCLUSION

We have discussed the general mathematical and physical meaning of QP wave functions in inhomogeneous systems. For the specific case of a molecule adsorbed on a metal surface,

we found that the QP states can differ qualitatively from the orbitals obtained within the standard independent-particle approximation as exemplified by the HF approximation. Using the *GW* method, it was shown that image charge interactions pull the QP frontier molecular orbitals towards the surface. In contrast, the HF single-particle orbitals remain delocalized and identical to those of the isolated molecule. These results are of importance for the modeling of energy level alignment and

electron transport across metal-molecule interfaces and should be observable by low-temperature scanning probe experiments on molecules on insulating substrates.

ACKNOWLEDGMENT

K.S.T. acknowledges support from the Danish Research Council's Sapere Aude program.

*thygesen@fysik.dtu.dk

¹G. Grosso and G. P. Parravicini, *Solid State Physics* (Academic Press, New York, 2003).

²W. Kohn and L. J. Sham, *Phys. Rev.* **140**, 1133 (1965).

³L. Hedin, *Phys. Rev.* **139**, A796 (1965).

⁴Strictly speaking, $\Sigma_{xc}(z)$ is a function of a *complex* energy. It is analytic in the upper and lower half-planes and has simple poles or branch cuts along the real axis defined by the excitation energies of the $N \pm 1$ particle system.⁵ When writing $\Sigma_{xc}(\varepsilon)$ we understand the limit $\Sigma_{xc}(\varepsilon + i0^+)$.

⁵F. Aryasetiawan and O. Gunnarsson, *Rep. Prog. Phys.* **61**, 237 (1998).

⁶M. S. Hybertsen and S. G. Louie, *Phys. Rev. B* **34**, 5390 (1986).

⁷M. van Schilfgaarde, T. Kotani, and S. V. Faleev, *Phys. Rev. B* **74**, 245125 (2006).

⁸M. Shishkin and G. Kresse, *Phys. Rev. B* **74**, 035101 (2006).

⁹P. Rinke, A. Qteish, J. Neugebauer, C. Freysoldt, and M. Scheffler, *New J. Phys.* **7**, 126 (2005).

¹⁰G. Onida, L. Reining, and A. Rubio, *Rev. Mod. Phys.* **74**, 601 (2002).

¹¹C. Rostgaard, K. W. Jacobsen, and K. S. Thygesen, *Phys. Rev. B* **81**, 085103 (2010).

¹²X. Blase, C. Attaccalite, and V. Olevano, *Phys. Rev. B* **83**, 115103 (2011).

¹³J. B. Neaton, M. S. Hybertsen, and S. G. Louie, *Phys. Rev. Lett.* **97**, 216405 (2006).

¹⁴J. M. Garcia-Lastra, C. Rostgaard, A. Rubio, and K. S. Thygesen, *Phys. Rev. B* **80**, 245427 (2009).

¹⁵K. S. Thygesen and A. Rubio, *Phys. Rev. Lett.* **102**, 046802 (2009).

¹⁶C. Freysoldt, P. Rinke, and M. Scheffler, *Phys. Rev. Lett.* **103**, 056803 (2009).

¹⁷A. Biller, I. Tamblyn, J. B. Neaton, and L. Kronik, *J. Chem. Phys.* **135**, 164706 (2011).

¹⁸S. Y. Quek, L. Venkataraman, H. J. Choi, S. G. Louie, M. S. Hybertsen, and J. B. Neaton, *Nano Lett.* **7**, 3477 (2007).

¹⁹D. J. Mowbray, G. Jones, and K. S. Thygesen, *J. Chem. Phys.* **128**, 111103 (2008).

²⁰M. Strange, C. Rostgaard, H. Hakkinen, and K. S. Thygesen, *Phys. Rev. B* **83**, 115108 (2011).

²¹M. Strange and K. S. Thygesen, *Beilstein J. Nanotechnol.* **2**, 746 (2011).

²²T. Rangel, A. Ferretti, P. E. Trevisanutto, V. Olevano, and G.-M. Rignanese, *Phys. Rev. B* **84**, 045426 (2011).

²³I. Tamblyn, P. Darancet, S. Y. Quek, S. A. Bonev, and J. B. Neaton, *Phys. Rev. B* **84**, 201402 (2011).

²⁴A. Ferretti, G. Mallia, L. Martin-Samos, G. Bussi, A. Ruini, B. Montanari, and N. M. Harrison, *Phys. Rev. B* **85**, 235105 (2012).

²⁵R. Pariser and R. G. Parr, *J. Chem. Phys.* **21**, 446 (1953); J. A. Pople, *Trans. Faraday Soc.* **42**, 1375 (1953).

²⁶K. Ohno, *Theor. Chim. Acta* **2**, 219 (1964).

²⁷W. Barford and R. J. Bursill, *Chem. Phys. Lett.* **268**, 535 (1997).

²⁸For completeness we briefly comment on the situation encountered for infinite systems. In this case Eq. (1) does not admit any exact solutions. Precisely, for ε belonging to the continuous spectrum, the eigenvalues, $E_i(\varepsilon)$, of the operator $[H_0 + \Sigma_{xc}(\varepsilon)]$ are complex, with a finite imaginary part. One can, however, define approximate solutions from the condition that $\text{Re}E_i(\varepsilon_i) = \varepsilon_i$.²⁹ These solutions represent a group of excitations and can be viewed as an average over states of the form defined in Eqs. (2) and (3) within an energy window around ε_i of width $\text{Im}E_i(\varepsilon_i)$. Solutions with a small $\text{Im}E_i(\varepsilon_i)$ represent well-defined excitations and will closely resemble the states in Eqs. (2) and (3).

²⁹L. J. Sham and W. Kohn, *Phys. Rev.* **145**, 561 (1966).

³⁰K. Kaasbjerg and K. S. Thygesen, *Phys. Rev. B* **81**, 085102 (2010).

³¹C. Verdozzi, R. W. Godby, and S. Holloway, *Phys. Rev. Lett.* **74**, 2327 (1995).

³²T. J. Pollehn, A. Schindlmayr, and R. W. Godby, *J. Phys.: Condens. Matter* **10**, 1273 (1998).

³³K. Kaasbjerg and K. Flensberg, *Nano Lett.* **8**, 3809 (2008).

³⁴R. Stadler, V. Geskin, and J. Cornil, *Phys. Rev. B* **79**, 113408 (2009).